Supporting Information

Systematic Comparison of Zwitterionic and Non-Zwitterionic Antifouling Polymer Brushes on a Bead-Based Platform

Esther van Andel,[a,b] *Stefanie C. Lange,*[a] *Sidharam P. Pujari,*[a] *Edwin J. Tijhaar,*[b] *Maarten M. J. Smulders,*[a] *Huub F. J. Savelkoul,*[b] *Han Zuilhof,*[a,c,d,*]

[a] Laboratory of Organic Chemistry, Wageningen University, Stippeneng 4, 6708 WE Wageningen, The Netherlands. [b] Cell Biology and Immunology group, Wageningen University, De Elst 1, 6709 PG Wageningen, The Netherlands. [c] School of Pharmaceutical Sciences and Technology, Tianjin University, 92 Weijin Road, Tianjin 300072, People's Republic of China. [d] Department of Chemical and Materials Engineering, King Abdulaziz University, Jeddah, Saudi Arabia

E-mail: Han.Zuilhof@wur.nl

TABLE OF CONTENTS

CHARACTERIZATION SYNTHESIZED MONOMERS

3-((3-methacrylamidopropyl)dimethylammonio)ethane-1-sulfonate (**SBMAA-2**)

Yield: 4.5 g (16 mmol, 56%), [$C_{11}H_{22}N_2O_4S$, M = 278.37 g/mol]

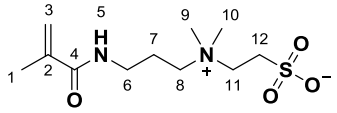

^{1}H NMR (400 MHz, D_2O) δ 5.62 (s, 1H, 3a), 5.37 (s, 1H, 3b), 3.65 – 3.55 (m, 2H, 11-H), 3.34 – 3.23 (m, 6H, 6,8,12-H), 3.05 (s, 6H, 9,10-H), 1.97 (dt, J = 14.9, 6.7 Hz, 2H, 7-H), 1.83 (s, 3H, 1-H) ppm.

^{13}C NMR (101 MHz, D_2O) δ 171.99 (C-4), 138.82 (C-2), 121.36 (C-3), 62.20 (C-8), 59.17 (C-11), 50.93 (C-9,10), 44.05 (C-6), 36.13 (C-12), 22.28 (C-7), 17.60 (C-1) ppm.

ESI$^+$ (MeOH): calc.: m/z = 301.1198 $[M+Na]^+$; det.: m/z = 301.1187 $[M+Na]^+$.

IR (ATR): ν = 3382 (w, N–H stretching), 3041 (w, asymmetric CH_2 stretching), 2947 (w, asymmetric CH_2 stretching), 1656 (m, C=O bending), 1614 (m, alkene stretching), 1524 (m, N–H bending), 1202 (s, SO_2 symmetric stretching), 1038 (s, SO_3 stretching) cm^{-1}.

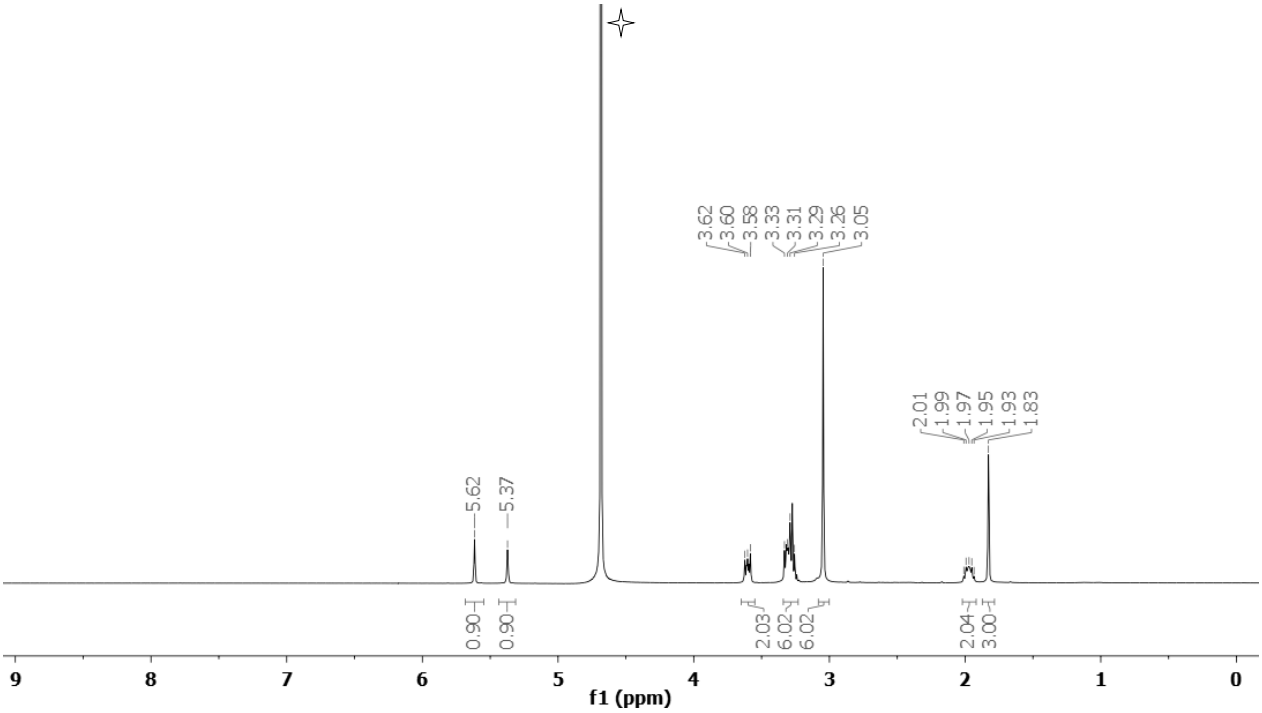

Figure S1. ^{1}H-NMR spectrum of **SMBAA-2** in D_2O at 300 K, 400 MHz. ✧ residual H_2O.

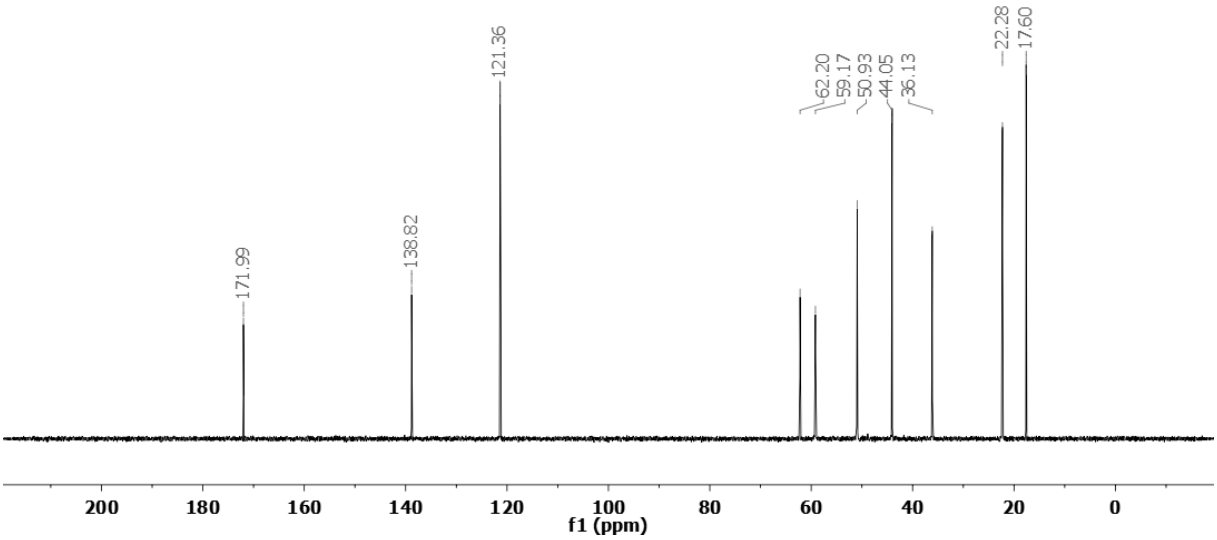

Figure S2. ^{13}C-NMR spectrum of **SBMAA-2** in D_2O at 300 K, 101 MHz.

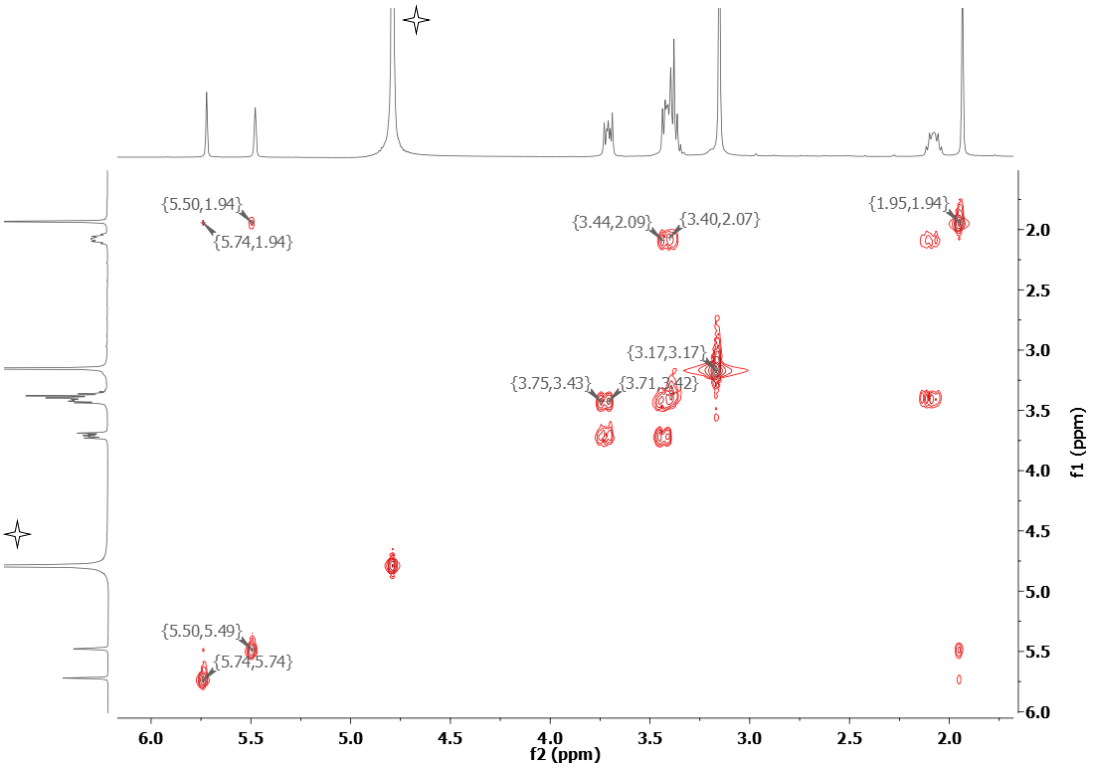

Figure S3. GCOSY-NMR spectrum of **SBMAA-2** in D_2O at 300 K, 400 MHz. ✧ residual H_2O.

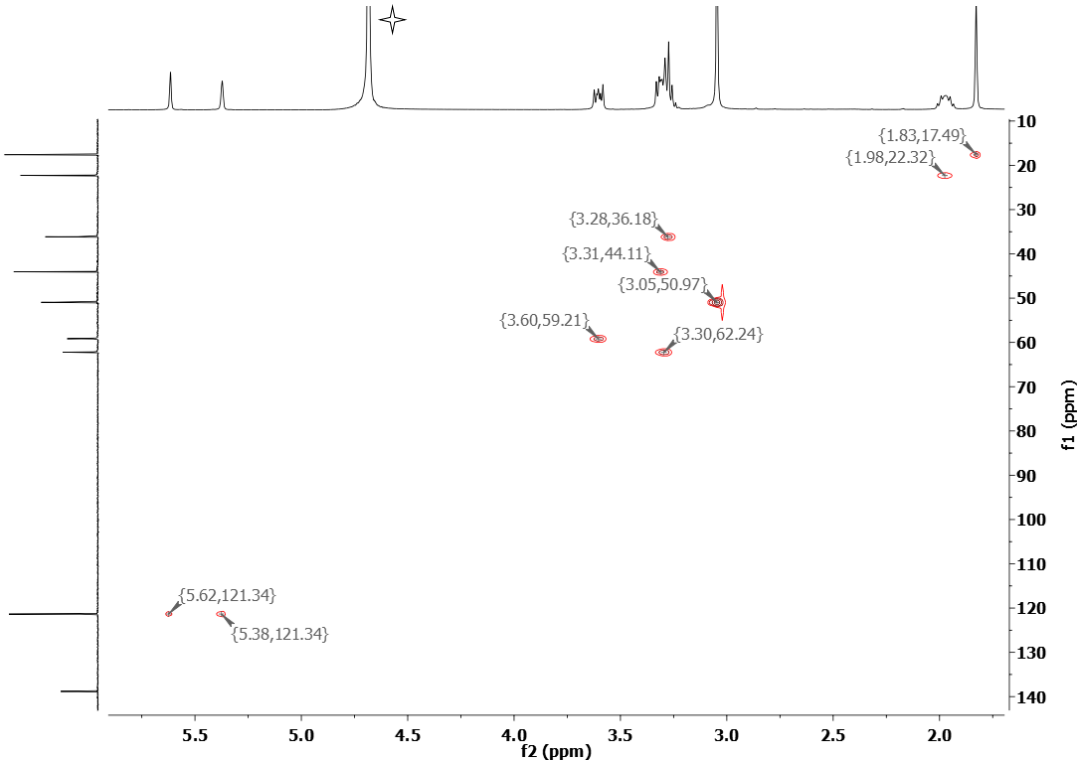

Figure S4. GHSQC-NMR spectrum of **SBMAA-2** in D_2O at 300 K, 400 MHz for ^{1}H-NMR and 101 MHz for ^{13}C-NMR. ✧ residual H_2O.

3-((3-methacrylamidopropyl)dimethylammonio)propane-1-sulfonate (**SBMAA-3**)[1]

Yield: 15.1 g (51.7 mmol, 94%), [$C_{12}H_{24}N_2O_4S$, M = 292.39 g/mol]

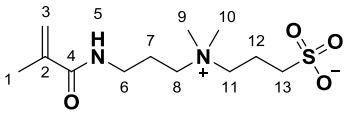

^{1}H NMR (400 MHz, D_2O) δ 5.68 (s, 1H, 3a-H), 5.44 (s, 1H, 3b-H), 3.49 – 3.40 (m, 2H, 11-H), 3.38 – 3.29 (m, 4H, 6,8-H), 3.08 (s, 6H, 9,10-H), 2.94 (t, J = 7.2 Hz, 2H, 13-H), 2.24 – 2.11 (m, 2H, 12-H), 2.07–1.96 (m, 2H, 7-H), 1.90 (s, 3H, 1-H) ppm.

^{13}C NMR (101 MHz, D_2O) δ 171.95 (C-4), 138.76 (C-2), 121.33 (C-3), 62.12 (C-11), 61.81 (C-8), 50.68 (C-9,10), 47.14 (C-13), 36.15 (C-6), 22.21 (C-7), 18.08 (C-12), 17.57 (C-1) ppm.

ESI$^+$ (MeOH): calc.: m/z = 293.1530 $[M+H]^+$, 315.1349 $[M+Na]^+$, 585.2986 $[2M+H]^+$, 607.2806 $[2M+Na]^+$; det.: m/z = 293.1515 $[M+H]^+$, 315.1332 $[M+Na]^+$, 585.2956 $[2M+H]^+$, 607.2774 $[2M+Na]^+$.

IR (ATR): ν = 3305 (w, N–H stretching), 3031 (w, asymmetric CH_2 stretching), 2977 (w, symmetric CH_2 stretching), 1656 (m, C=O bending), 1614 (m, alkene stretching), 1546 (m, N–H bending), 1191-1174 (s, SO_2 symmetric stretching), 1038 (s, SO_3 stretching) cm^{-1}.

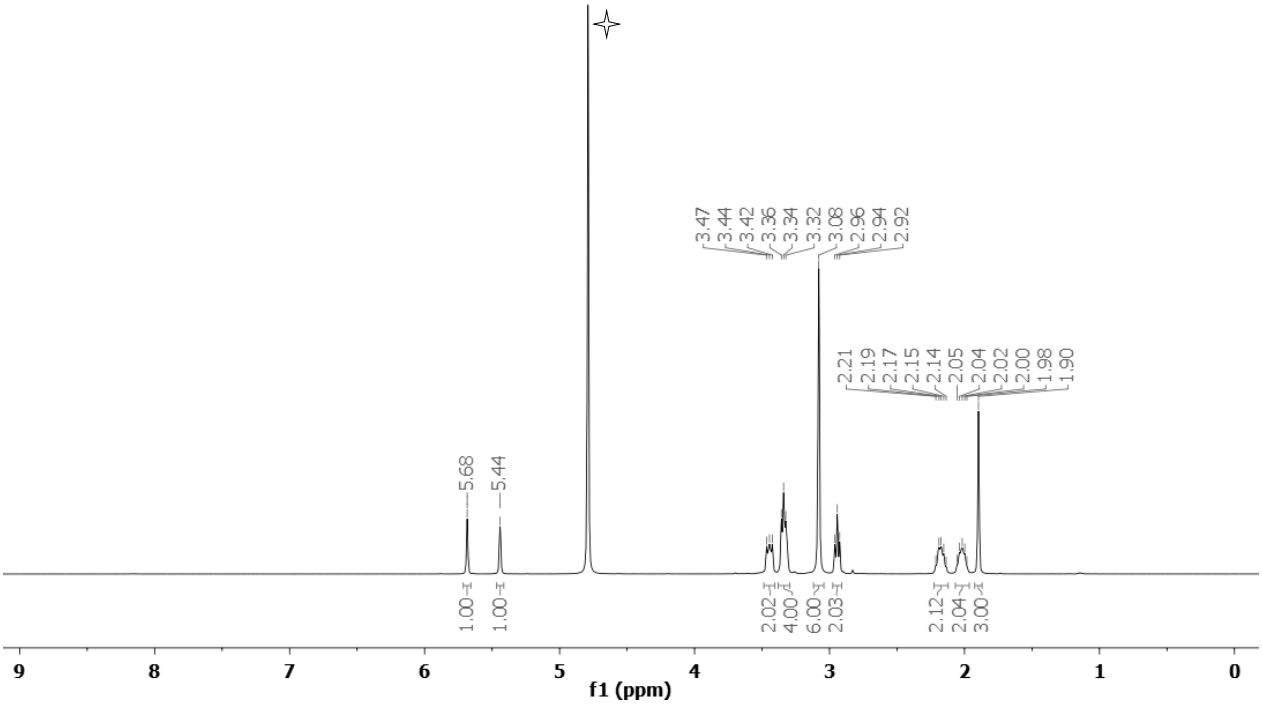

Figure S5. ^{1}H-NMR spectrum of **SBMAA-3** in D_2O at 300 K, 400 MHz. ✧ residual H_2O.

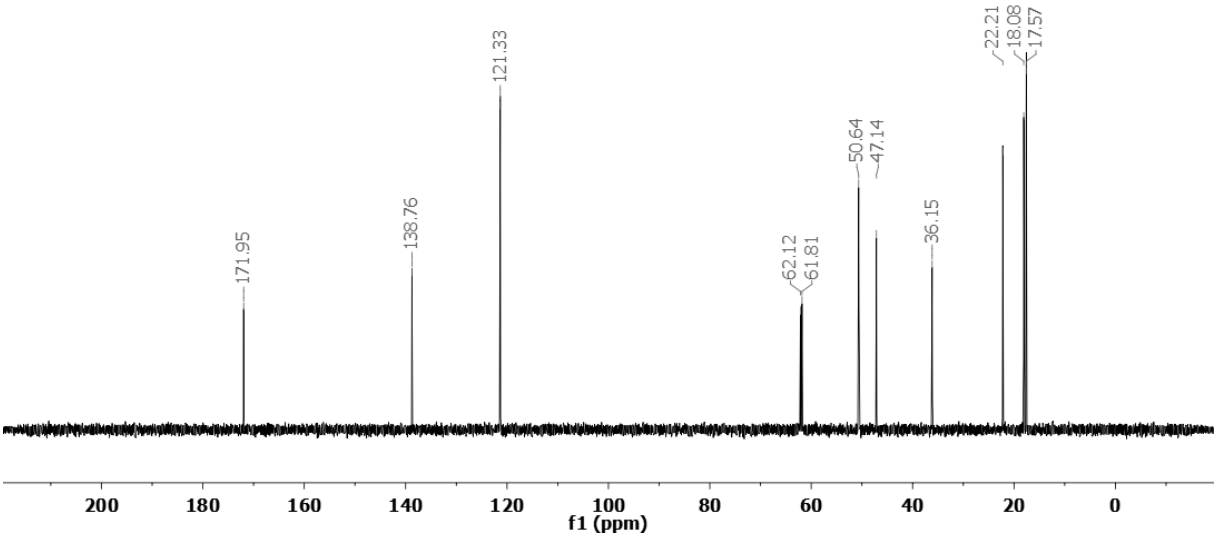

Figure S6. ^{13}C-NMR spectrum of **SBMAA-3** in D_2O at 300 K, 101 MHz.

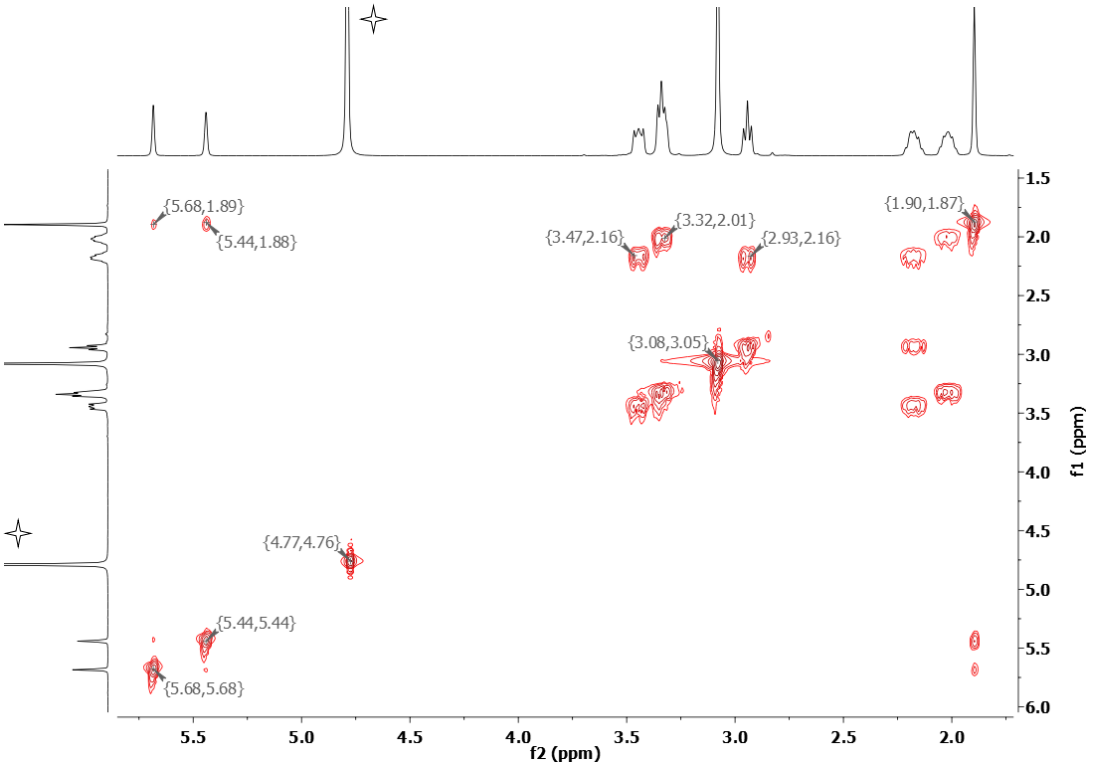

Figure S7. GCOSY-NMR spectrum of **SBMAA-3** in D_2O at 300 K, 400 MHz. ✧residual H_2O.

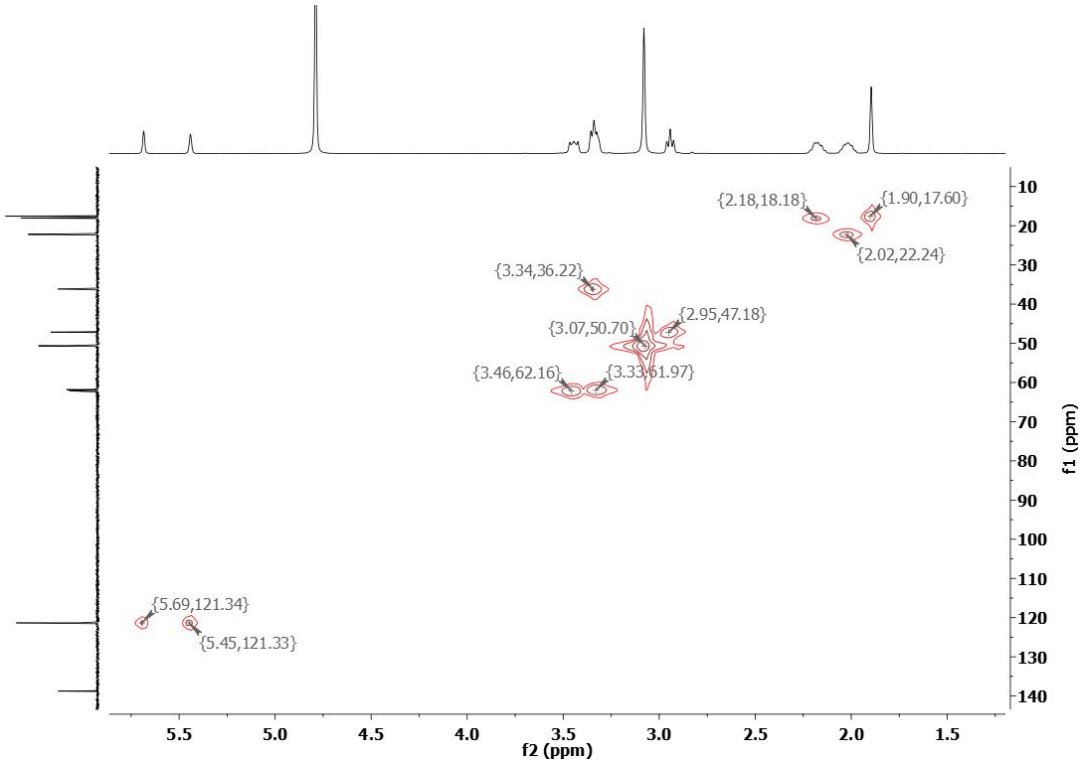

Figure S8. GHSQC-NMR spectrum of **SBMAA-3** in D_2O at 300 K, 400 MHz for ^{1}H-NMR and 101 MHz for ^{13}C-NMR. ✧residual H_2O.

3-((3-methacrylamidopropyl)dimethylammonio)propanoate (CBMAA-2)

Yield: 30.0 g (124 mmol, 45%), [$C_{12}H_{22}N_2O_3$, M = 242.32 g/mol]

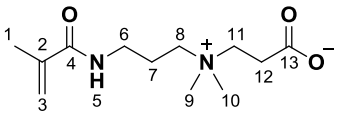

^{1}H NMR (400 MHz, D_2O) δ 5.63 (s, 1H, 3a-H), 5.39 (s, 1H, 3b-H), 3.48 (t, J = 7.8 Hz, 2H, 6-H), 3.32 – 3.20 (m, 4H, 8,11-H), 2.99 (s, 6H, 9,10-H), 2.62 – 2.52 (m, 2H, 12-H), 2.03 – 1.90 (m, 2H, 7-H), 1.84 (d, J = 1.2 Hz, 3H, 1-H) ppm.

^{13}C NMR (101 MHz, D_2O) δ 176.53 (C-13), 172.03 (C-4), 138.81 (C-2), 121.29 (C-3), 61.93 (C-11), 61.19 (C-8), 50.55-50.46 (C-9,10), 36.19 (C-6), 30.71 (C-12), 22.22 (C-7), 17.56 (C-1) ppm.

ESI$^+$ (MeOH): calc.: m/z = 243.1703 $[M+H]^+$, 265.1523 $[M+Na]^+$; det: m/z = 243.1698 $[M+H]^+$, 265.1517 $[M+Na]^+$.

IR (ATR): ν = 3284 (m, carboxylate), 3037 (w, asymmetric CH_2 stretching), 2957 (w, symmetric CH_2 stretching), 1734 (w, carboxylic acid C=O bending), 1658 (m, amide C=O bending), 1591 (s, alkene stretching), 1540 (s, N–H bending) cm^{-1}.

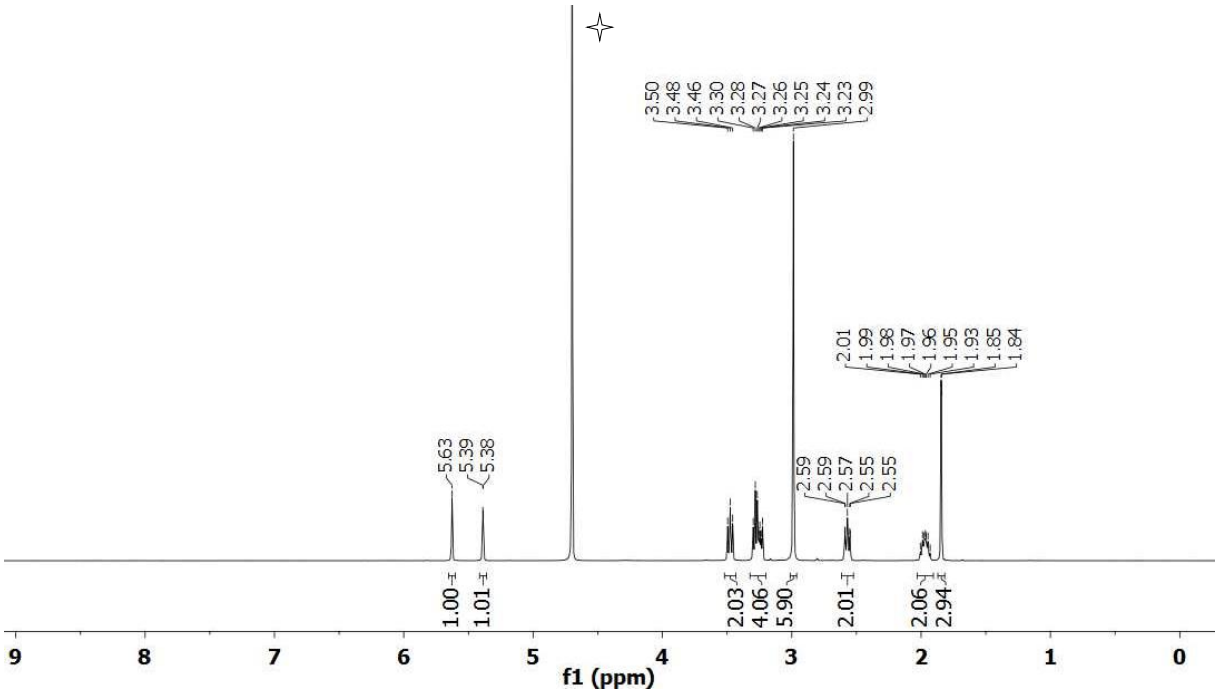

Figure S9. ^{1}H-NMR spectrum of **CBMAA-2** in D_2O at 300 K, 400 MHz. ✧ residual H_2O.

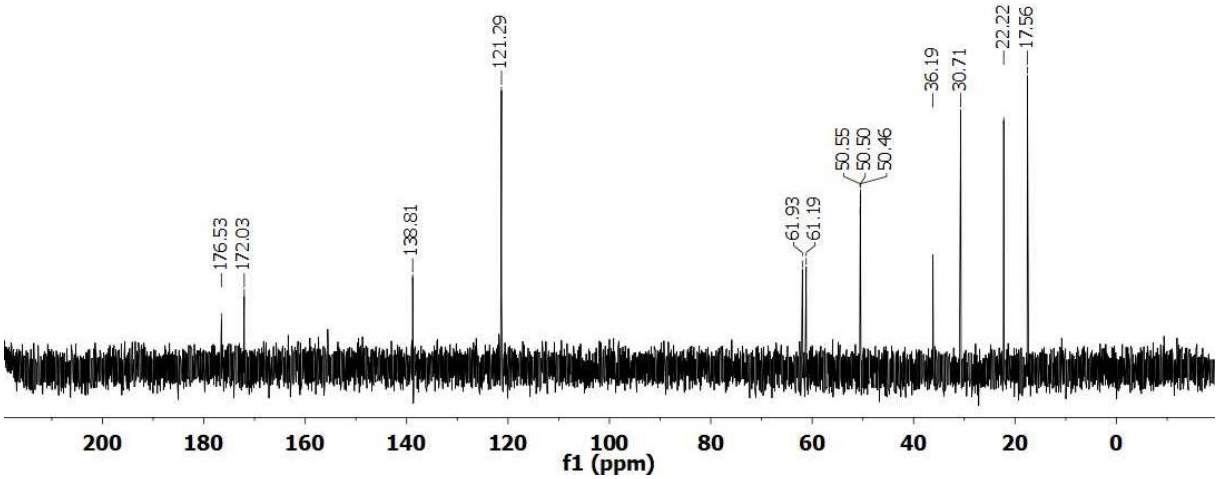

Figure S10: ^{13}C-NMR spectra of **CBMAA-2** in D_2O at 300 K, 101 MHz.

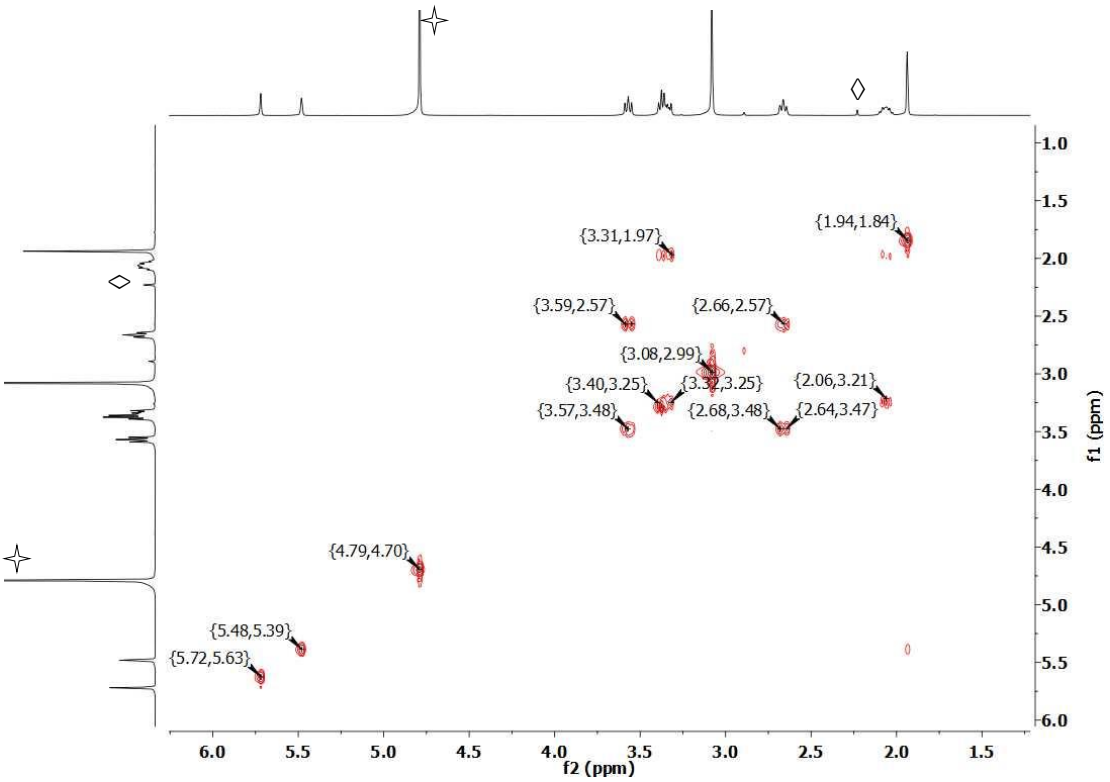

Figure S11. GCOSY-NMR spectrum of **CBMAA-2** in D_2O at 300 K, 400 MHz. ✧ residual H_2O, ◊ residual acetone.

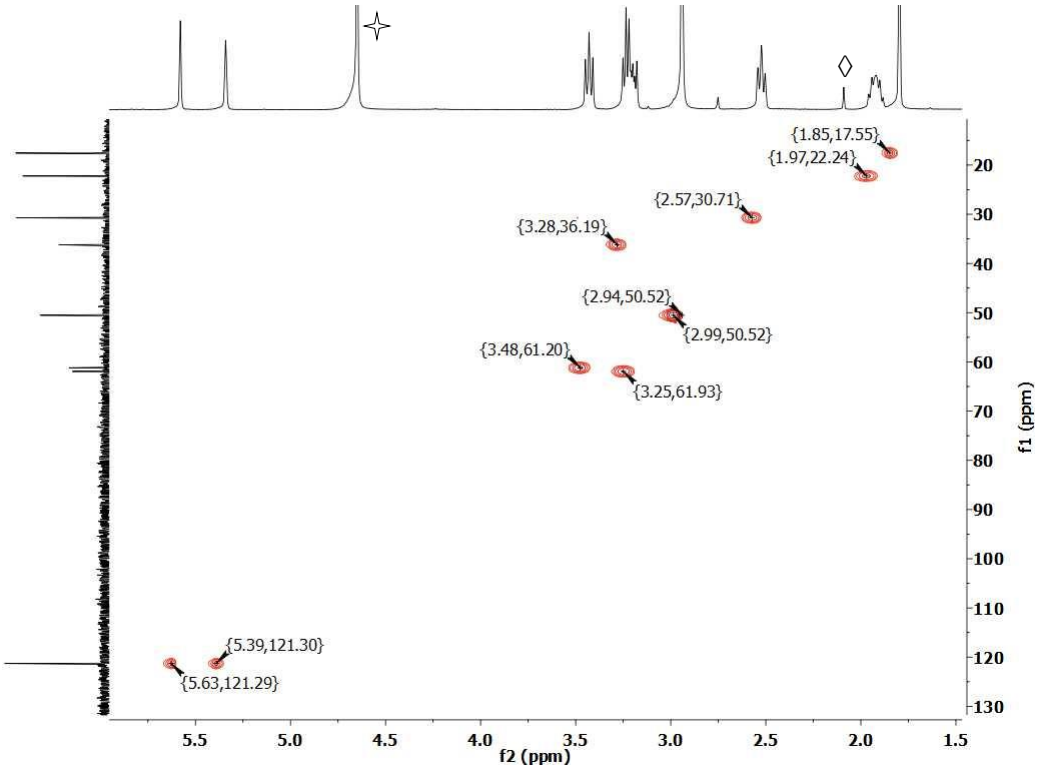

Figure S12. GHSQC-NMR spectrum of **CBMAA-2** in D_2O at 300 K, 400 MHz for ^{1}H-NMR and 101 MHz for ^{13}C-NMR. ✧ residual H_2O, ◊ residual acetone.

ADDITIONAL XPS SPECTRA

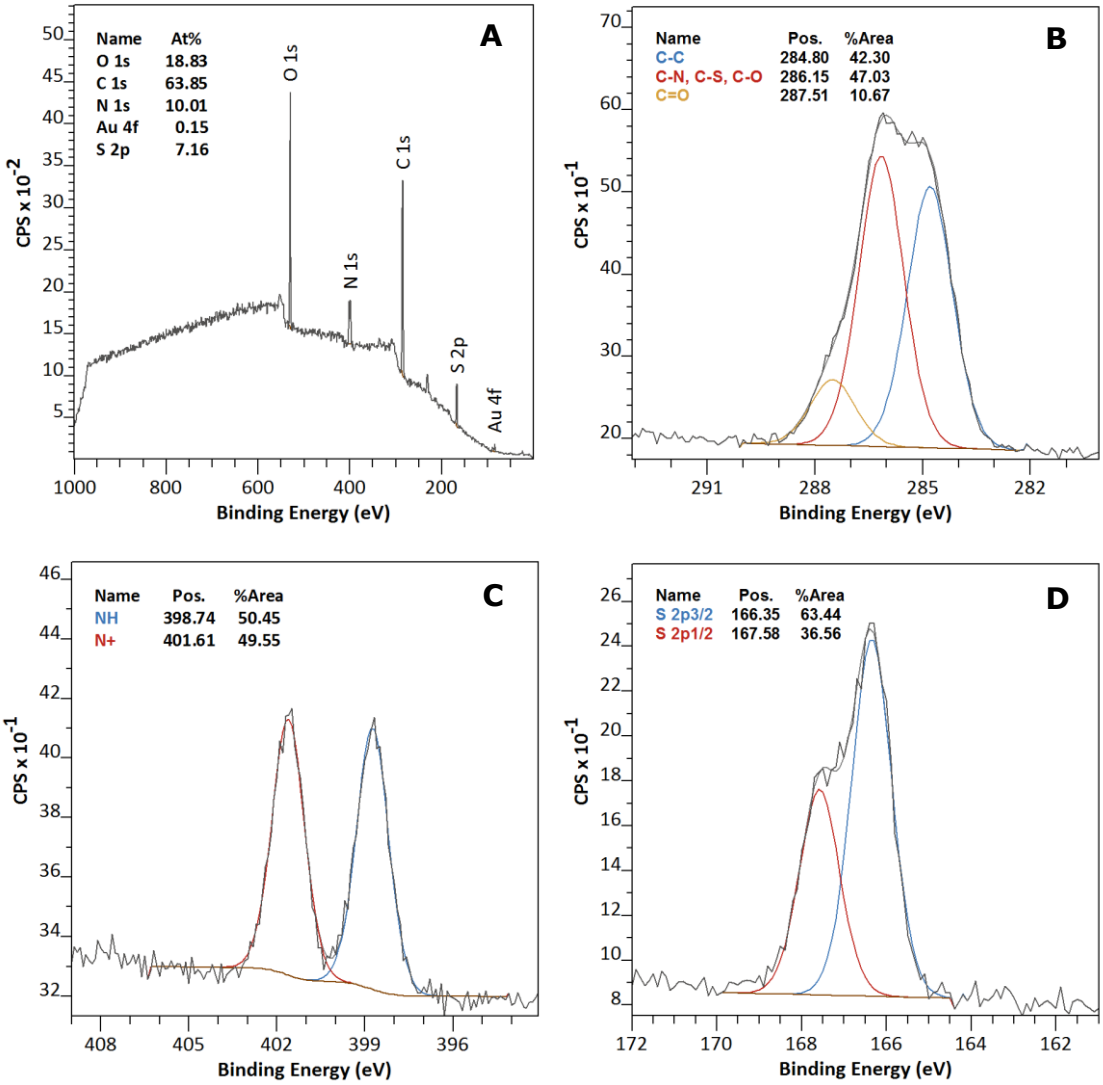

Figure S13. XPS spectra of gold surfaces coated with **SBMAA-2** polymer brushes grown via SI-ATRP: (A) wide scan spectrum, (B) C 1s narrow scan spectrum, (C) N 1s narrow scan spectrum and (D) S 2p narrow scan spectrum.

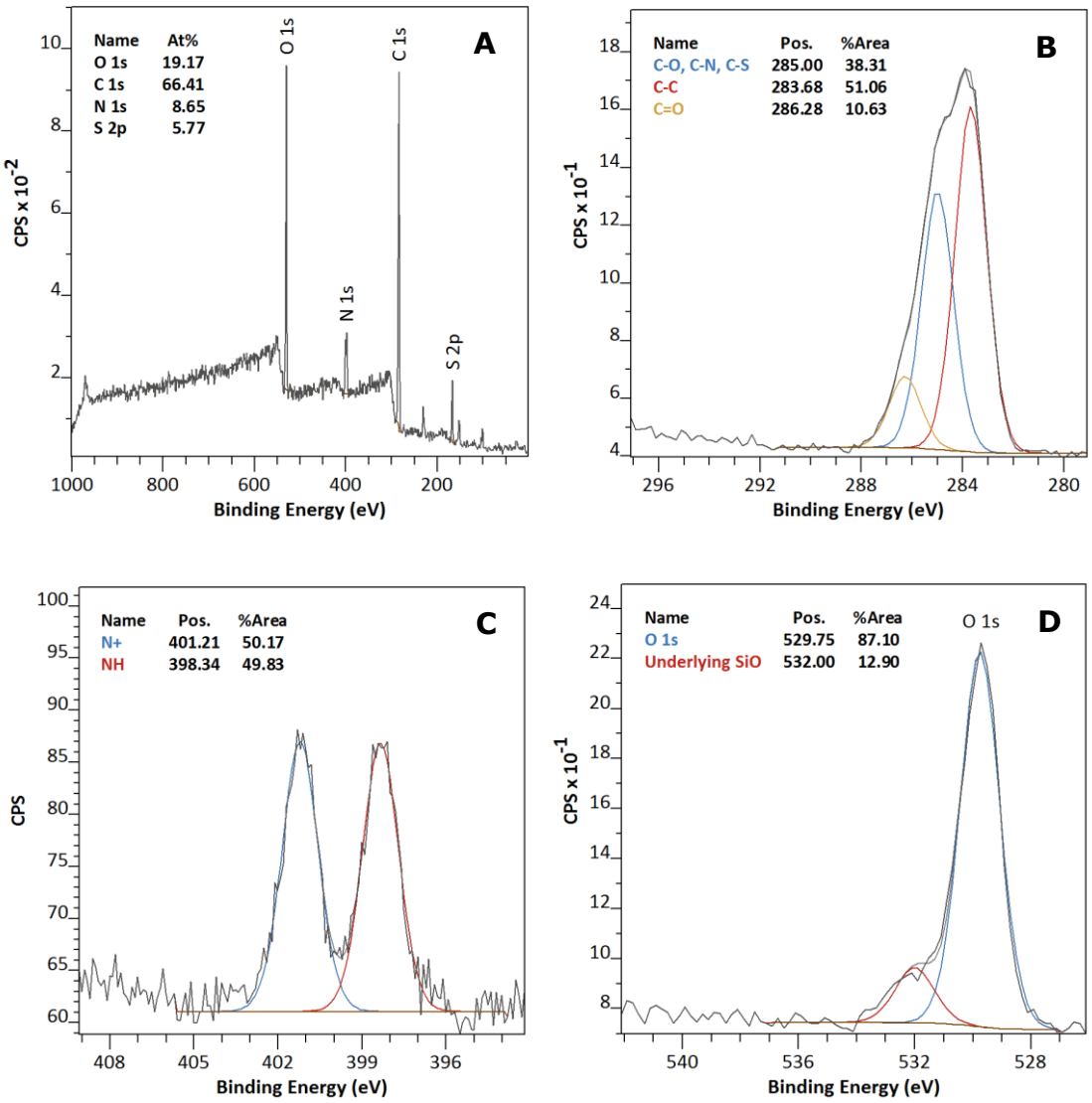

Figure S14. XPS spectra of Dynabeads modified with **SBMAA-2** polymer brushes grown via SI-ATRP: (A) wide scan spectrum, (B) C 1s narrow scan spectrum, (C) N 1s narrow scan spectrum and (D) O 1s narrow scan spectrum. **SBMAA-2**-coated Dynabeads were dropcasted on a Si(111) surface to allow for XPS analysis. *The two extra peaks (to the right of the S 2p peak) in the wide scans and the minor oxygen peak in thw oxygen narrow scan spectrum originate from the underlying SiO layer.

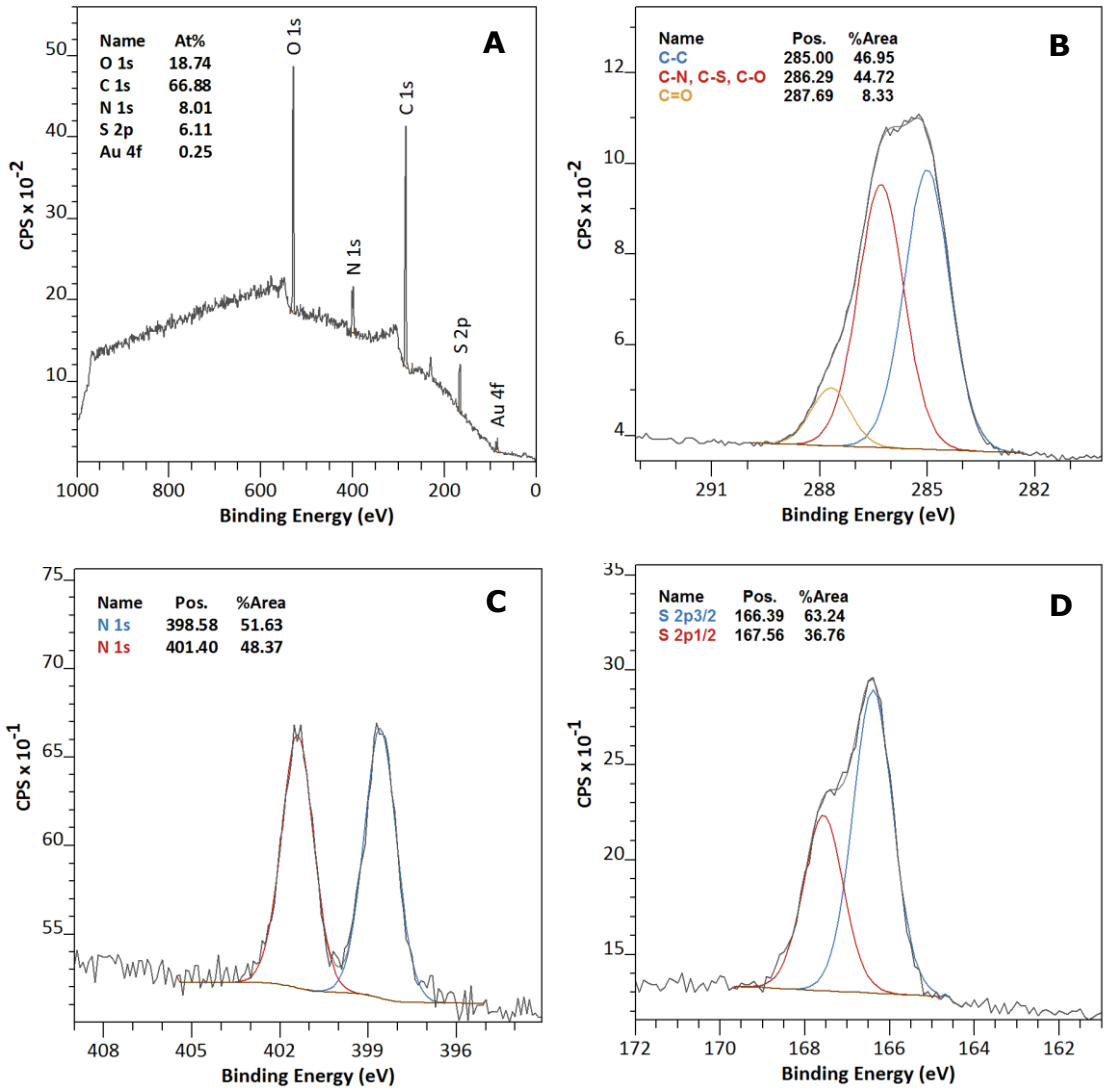

Figure S15. XPS spectra of gold surfaces coated with **SBMAA-3** polymer brushes grown via SI-ATRP: (A) wide scan spectrum, (B) C 1s narrow scan spectrum, (C) N 1s narrow scan spectrum and (D) S 2p narrow scan spectrum.

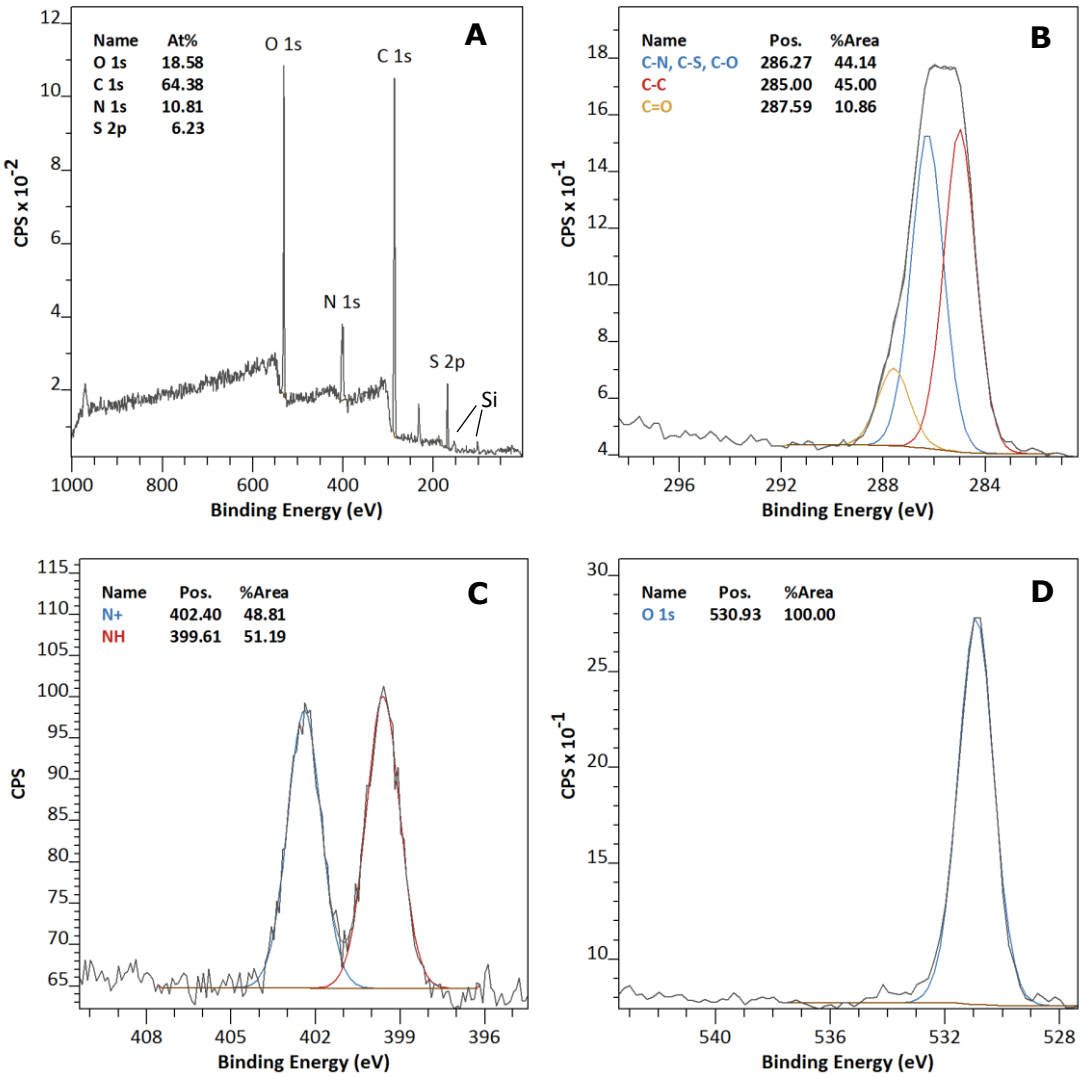

Figure S16. XPS spectra of Dynabeads modified with **SBMAA-3** polymer brushes grown via SI-ATRP: (A) wide scan spectrum, (B) C 1s narrow scan spectrum, (C) N 1s narrow scan spectrum and (D) O 1s narrow scan spectrum. **SBMAA-3**-coated Dynabeads were dropcasted on a Si(111) surface to allow for XPS analysis (hence the small Si peaks in the wide scan spectrum).

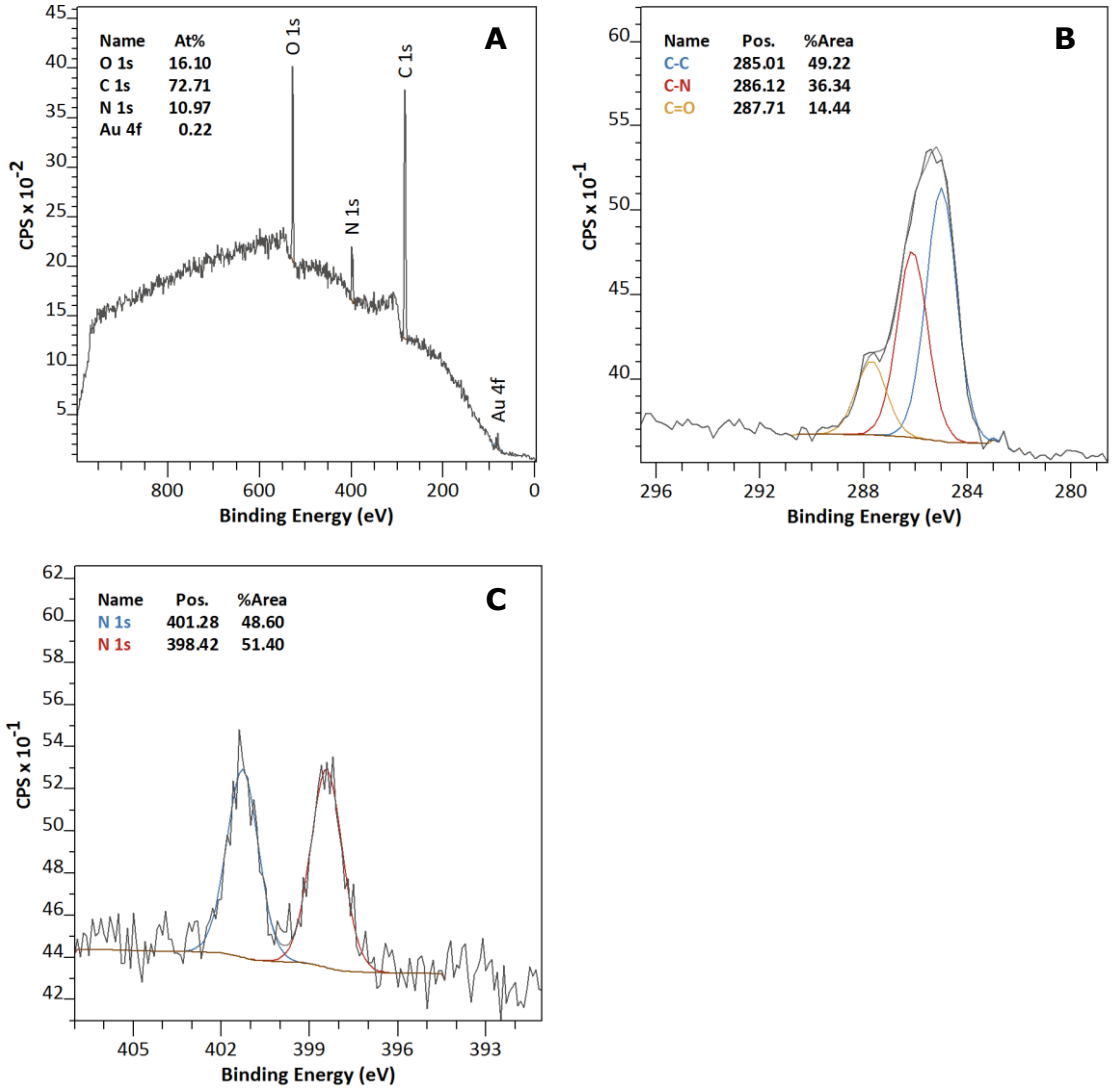

Figure S17. XPS spectra of gold surfaces coated with **CBMAA-2** polymer brushes grown via SI-ATRP: (A) wide scan spectrum and (B) N 1s narrow scan spectrum.

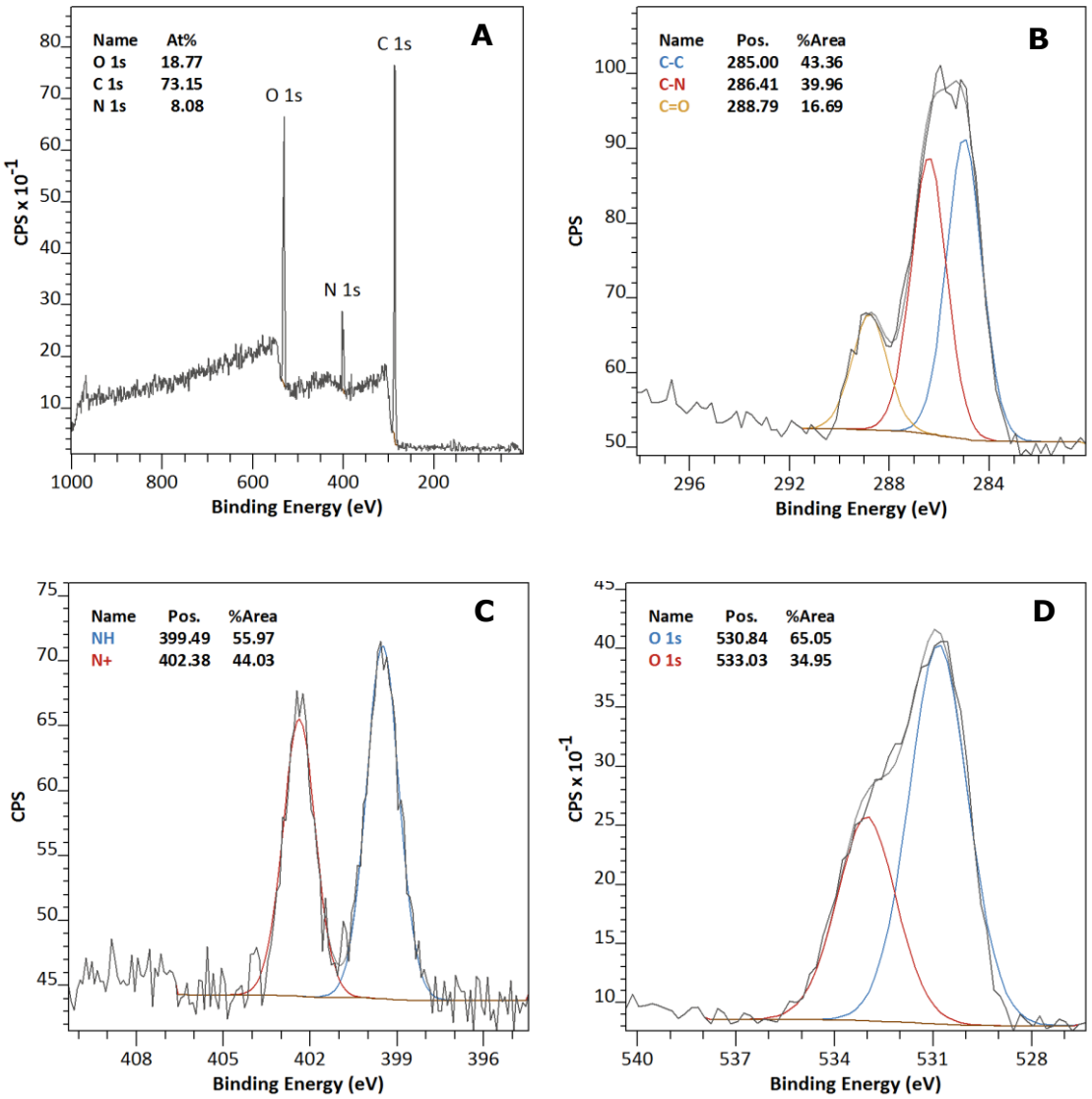

Figure S18. XPS spectra of Dynabeads modified with **CBMAA-2** polymer brushes grown via SI-ATRP: (A) wide scan spectrum, (B) C 1s narrow scan spectrum, (C) N 1s narrow scan spectrum and (D) O 1s narrow scan spectrum. **CBMAA-2**-coated Dynabeads were dropcasted on a Si(111) surface to allow for XPS analysis.

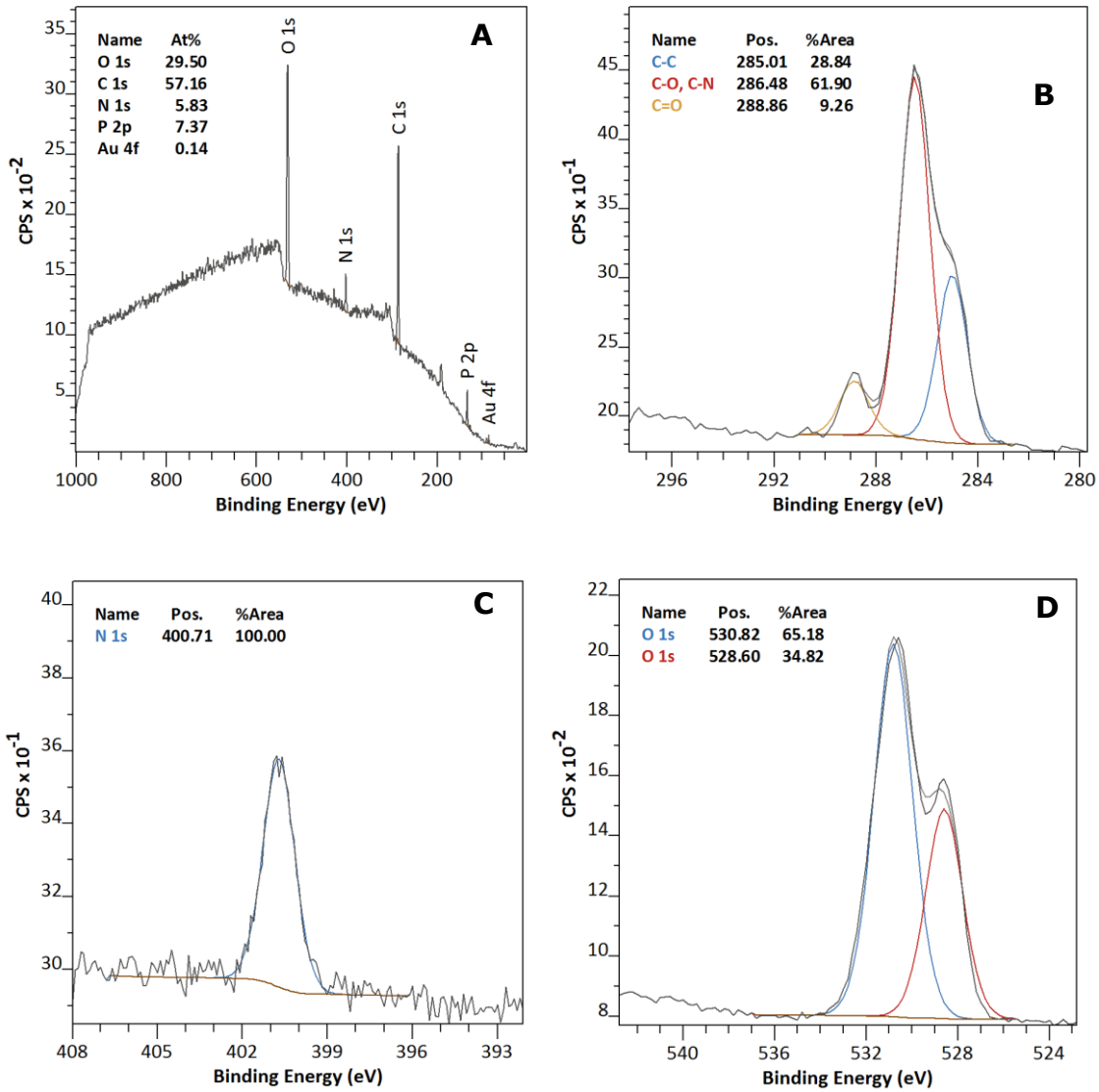

Figure S19. XPS spectra of gold surfaces coated with **PCMA-2** polymer brushes grown via SI-ATRP: (A) wide scan spectrum, (B) C 1s narrow scan spectrum, (C) N 1s narrow scan spectrum and (D) O 1s narrow scan spectrum.

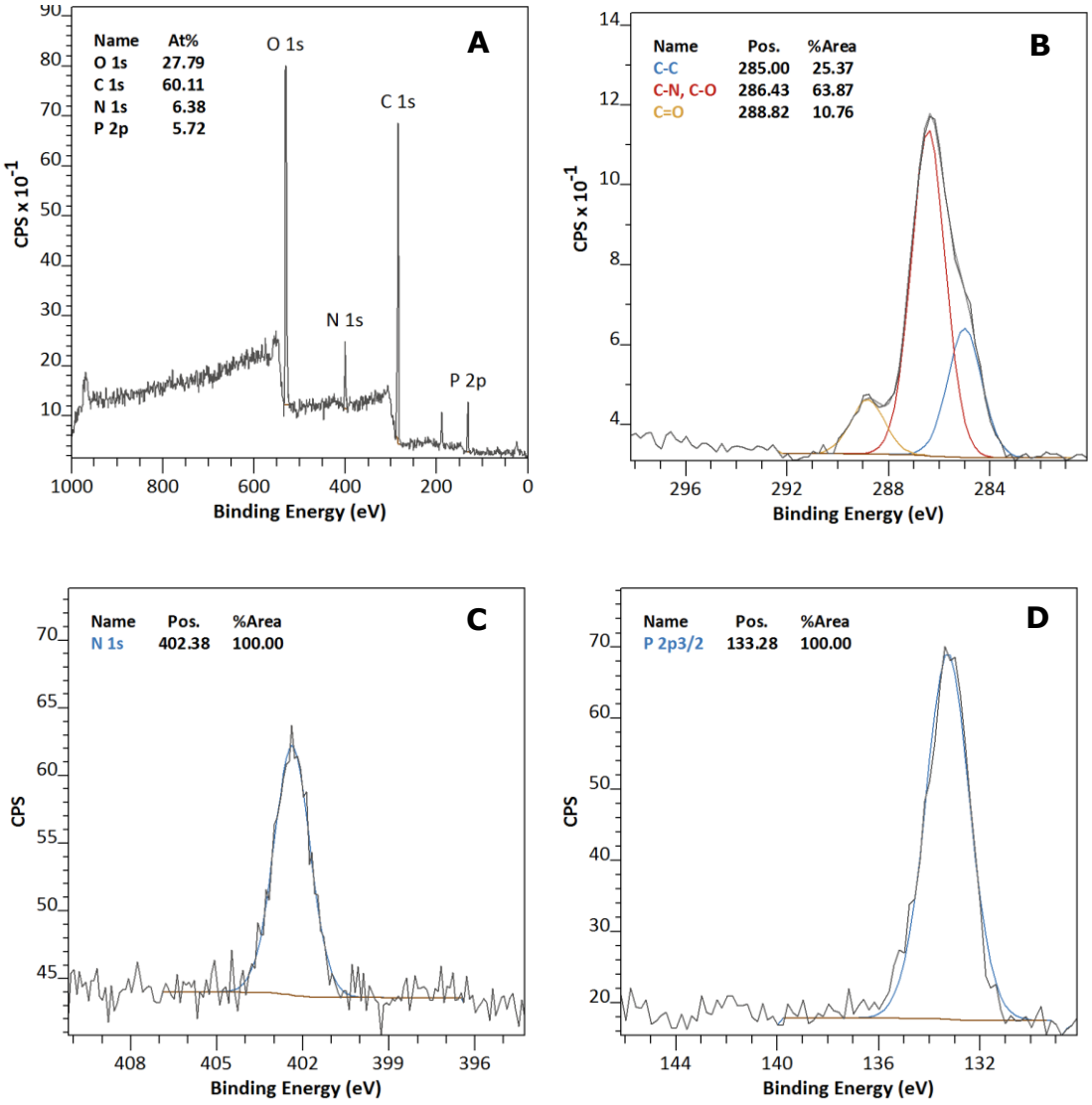

Figure S20. XPS spectra of Dynabeads modified with **PCMA-2** polymer brushes grown via SI-ATRP: (A) wide scan spectrum, (B) C 1s narrow scan spectrum, (C) N 1s narrow scan spectrum and (D) P 2p narrow scan spectrum and (E). **PCMA-2**-coated Dynabeads were dropcasted on a Si(111) surface to allow for XPS analysis.

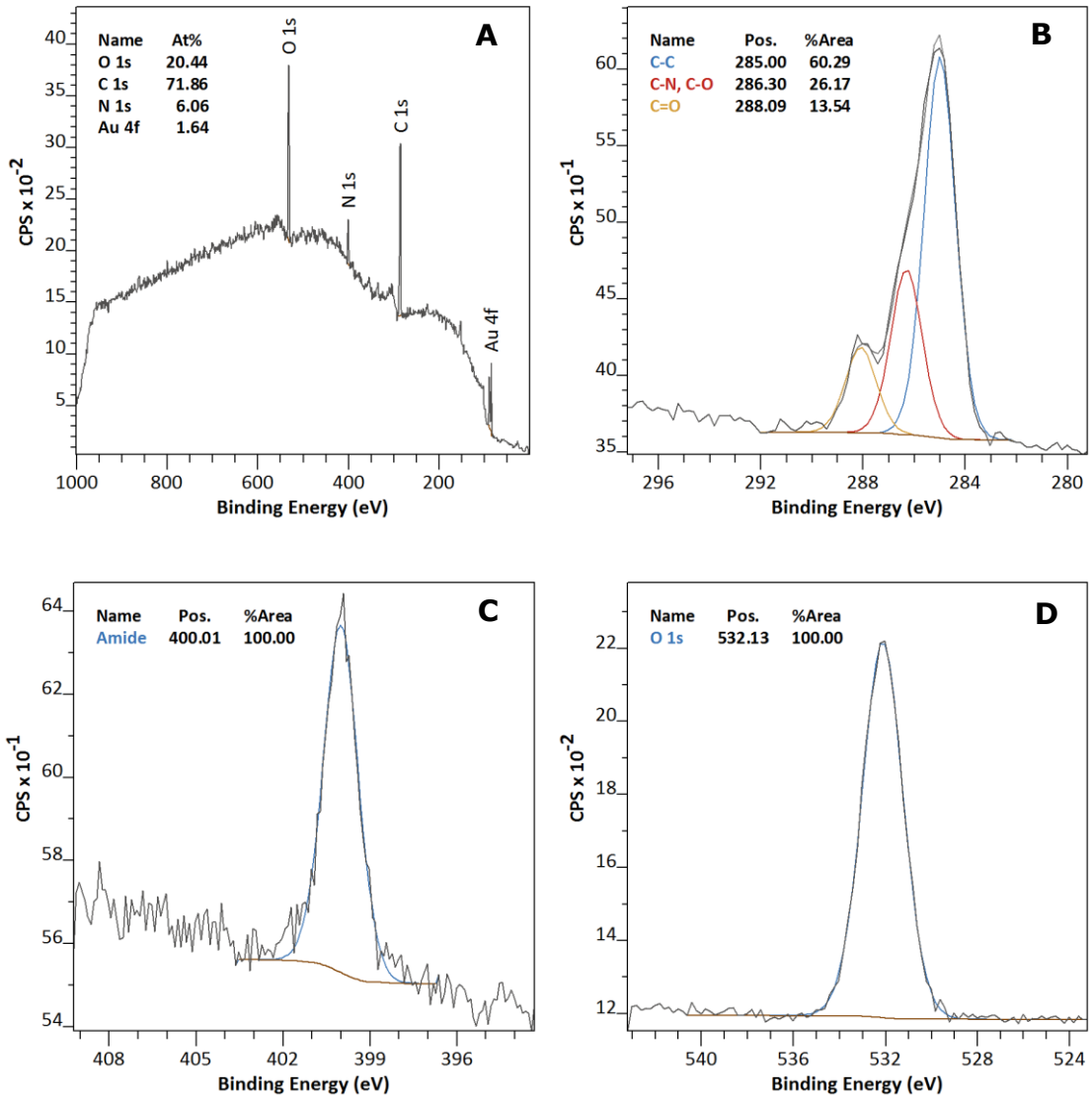

Figure S21. XPS spectra of gold surfaces coated with **HPMAA** polymer brushes grown via SI-ATRP: (A) wide scan spectrum, (B) C 1s narrow scan spectrum, (C) N 1s narrow scan spectrum and (D) O 1s narrow scan spectrum.

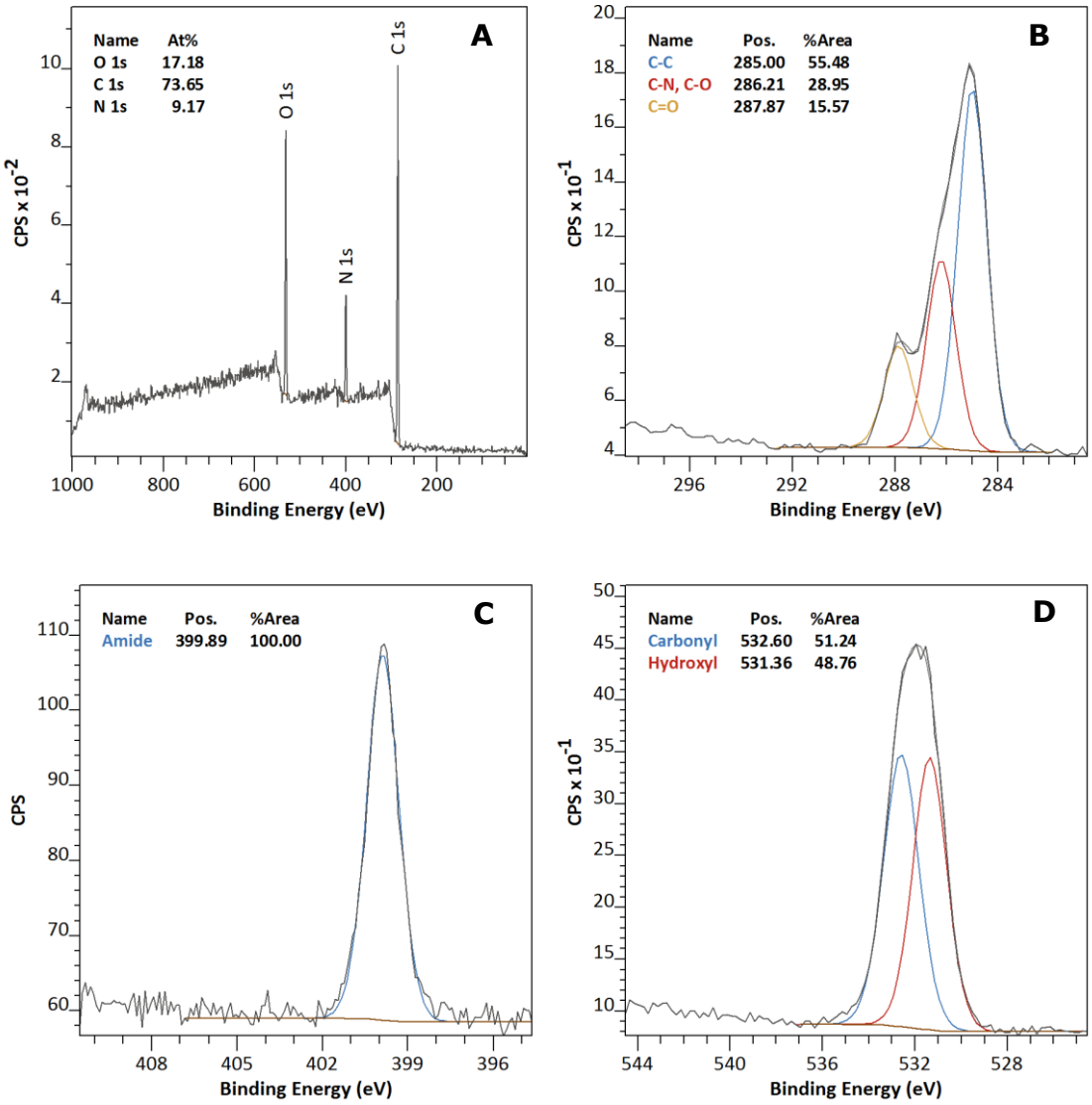

Figure S22. XPS spectra of Dynabeads modified with **HPMAA** polymer brushes grown via SI-ATRP: (A) wide scan spectrum, (B) C 1s narrow scan spectrum, (C) N 1s narrow scan spectrum and (D) O 1s narrow scan spectrum. Poly(**HPMAA**)-coated Dynabeads were dropcasted on a Si(111) surface to allow for XPS analysis.

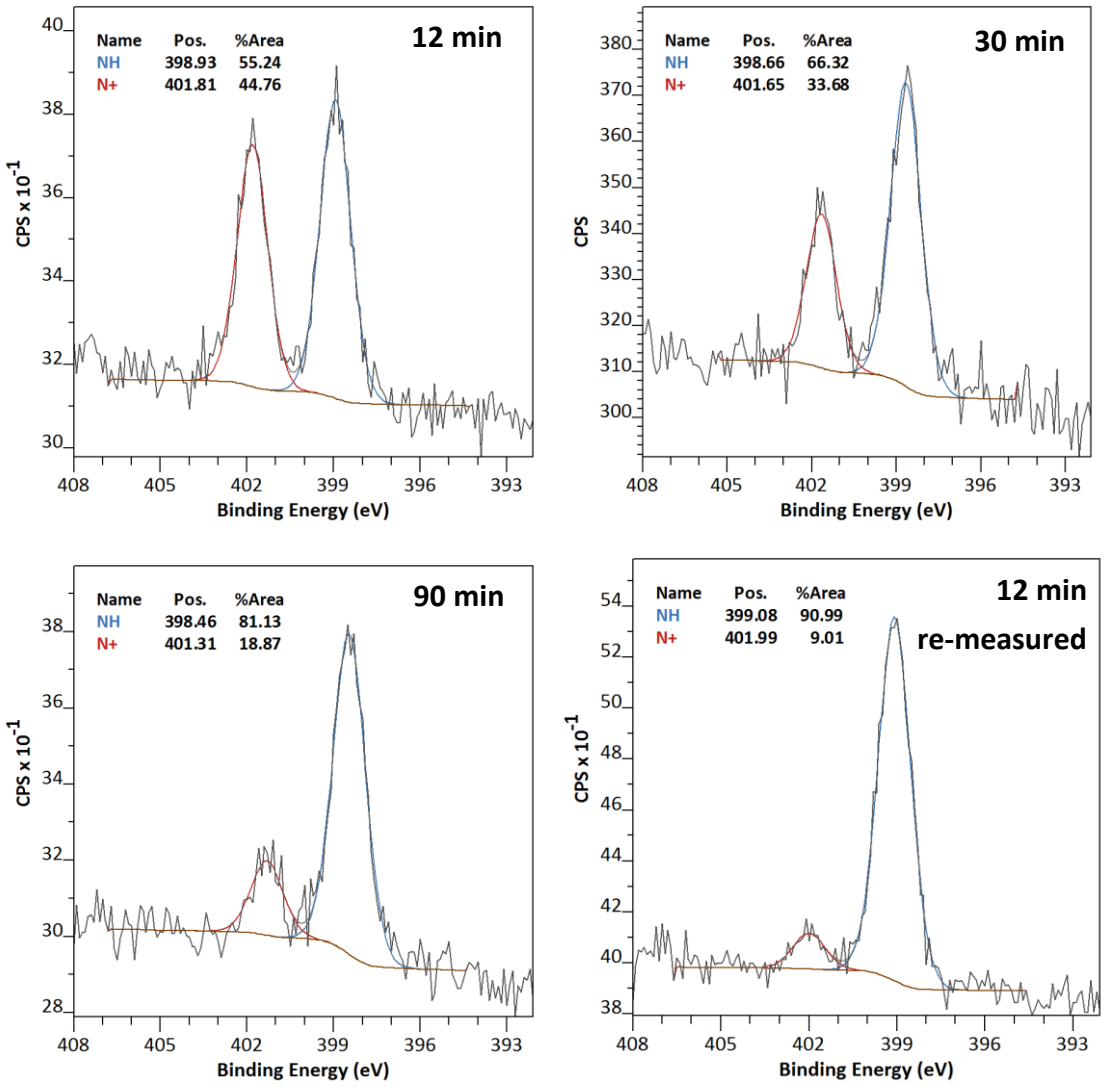

Figure S23. XPS N 1s narrow scan spectra of poly(**CBMAA-2**)-coated gold surfaces grown via SI-ATRP for 12, 30 and 90 min. The surfaces were placed together inside the XPS chamber and measured sequentially in the order of 12, 30 and 90 min ATRP. Without having taken the samples out of the XPS, the 12 min gold surface was measured again. These data revealed that the time within the XPS chamber determines the relative heights of the N 1s peaks.

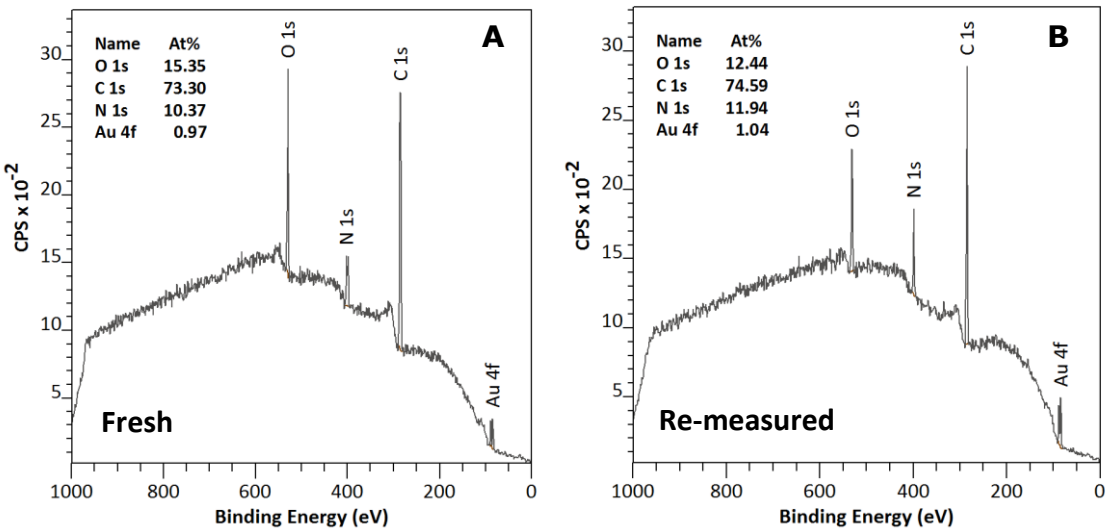

Figure S24. XPS wide scan spectra of a poly(**CBMAA-2**)-coated gold surface prepared by 12 min SI-ATRP: either measured directly (A) or after approximately 12 hours (B) without having taken the sample out of the XPS.

ZETA POTENTIAL MEASUREMENTS

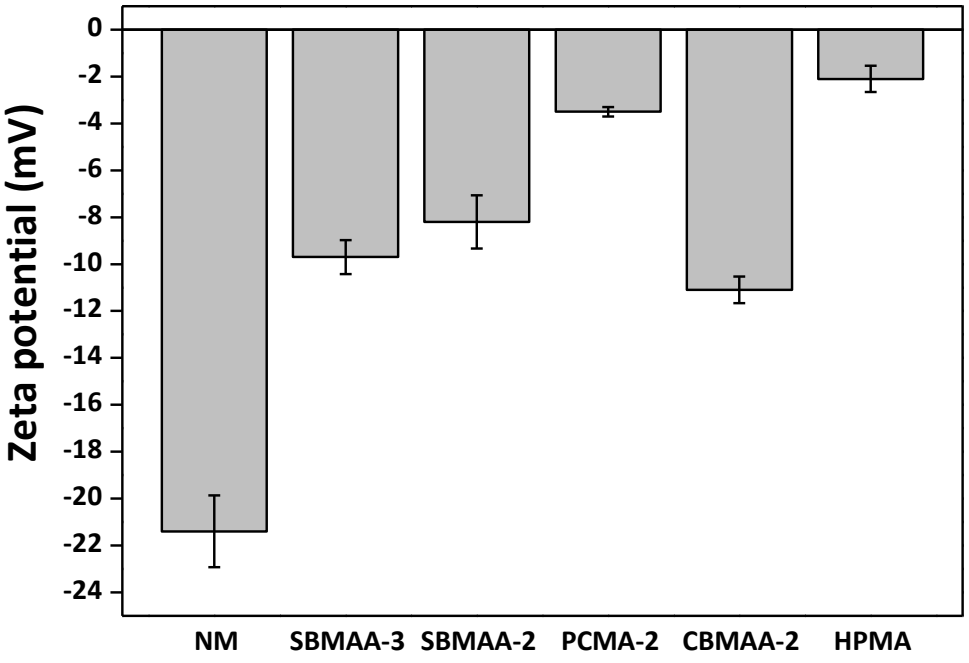

Figure S25. Zeta potentials of non-modified (NM) and polymer-coated Dynabeads, measured in PBS pH 7.4 at 25 °C. Presented data are averages of two independent measurements, standard deviations are presented as error bars. *NM beads showed positive zeta potentials in milliQ (30.6 ± 0.7) whereas all polymer-coated beads were negative in milliQ.

ADDITIONAL FLOW CYTOMETRY DATA

Table S1. Median fluorescence data (FITC-channel) obtained for non-modified and polymer-coated beads incubated in PBS or BSA-AF488 (0.5 mg/mL in PBS). PBS values are subtracted from BSA values to obtain the corrected values. The listed averages and standard deviations are used for Figure 4.

Sample	***PBS***	***BSA***	***Corrected value***	***Average***	***Standard deviation***
Non-modified	208	2409	2201		
	163	1967	1804		
	160	2782	2622	2209.0	409.1
SBMAA-3	312	321	9		
	253	258	5	7.0	2.8
SBMAA-2	318	336	18		
	256	273	17	17.5	0.7
CBMAA-2	210	221	11		
	229	246	17	14.0	4.2
PCMA-2	310	311	1		
	244	257	13	7.0	8.5
HPMAA	311	318	7		
	253	261	8	7.5	0.7

Table S2. Median fluorescence data (PE-channel) obtained for non-modified and polymer-coated beads incubated in PBS or biotinylated serum (~6 mg/mL) followed by Strep-PE. PBS values are subtracted from values for serum to obtain the corrected values. The listed averages and standard deviations are used for Figure 4.

Sample	*PBS*	*Serum*	*Corrected value*	*Average*	*Standard deviation*
Non-modified	95.7	8980	8884.3		
	97.5	9915	9817.5		
	95.1	8430	8334.9	9012.2	749.5
SBMAA-3	121	644	523		
	135	655	520	521.5	2.1
SBMAA-2	130	344	214		
	121	266	145		
	135	332	197	185.3	35.9
CBMAA-2	115	142	27		
	121	205	84	55.5	40.3
PCMA-2	129	171	42		
	121	185	64		
	133	226	93	66.3	25.6
HPMAA	129	155	26		
	121	154	33		
	134	181	47	35.3	10.7

SPR EXPERIMENTS

During our SPR experiments using sulfobetaine-coated surfaces, we observed a negative dip in the relative response units just after sample injection. The signal only stabilized after an extended time of flushing with running buffer. The dip was attributed to by the difference in salt concentration between running buffer and sample. This is supported by a similar dip that was observed when we injected buffer with an increased salt concentration (see Fig. S23). No dip was observed when a sucrose solution was with equal salt concentration between sample and running buffer. The dip is probably caused by a sudden swelling of the brushes caused by a difference in salt concentration between serum and the running buffer. Sulfobetaine-based materials swell considerably with increased ionic strength[2, 3] and as the refractive index lowers upon swelling,[4] a decrease in signal can be observed. To avoid salt effects, 100% bovine serum (pooled from 3 adult cows) was dialyzed against the running buffer. The serum dilutions were prepared from the dialyzed serum solution. Long injection times and low flow rates were needed in order to get enough fouling to be able to discriminate **SBMAA-3** from **SBMAA-2**.

REFERENCES

S1. Chen, L.; Honma, Y.; Mizutani, T.; Liaw, D. J.; Gong, J. P.; Osada, Y. Effects of polyelectrolyte complexation on the UCST of zwitterionic polymer. *Polymer* **2000,** *41* (1), 141-147.
S2. Higaki, Y.; Inutsuka, Y.; Sakamaki, T.; Terayama, Y.; Takenaka, A.; Higaki, K.; Yamada, N. L.; Moriwaki, T.; Ikemoto, Y.; Takahara, A. Effect of Charged Group Spacer Length on Hydration State in Zwitterionic Poly(sulfobetaine) Brushes. *Langmuir* **2017,** *33* (34), 8404-8412.
S3. Wang, T.; Kou, R.; Liu, H.; Liu, L.; Zhang, G.; Liu, G. Anion Specificity of Polyzwitterionic Brushes with Different Carbon Spacer Lengths and Its Application for Controlling Protein Adsorption. *Langmuir* **2016,** *32* (11), 2698-2707.
S4. Tang, Y.; Lu, J. R.; Lewis, A. L.; Vick, T. A.; Stratford, P. W. Swelling of zwitterionic polymer films characterized by spectroscopic ellipsometry. *Macromolecules* **2001,** *34* (25), 8768-8776.